



HAL
open science

Learning a weather dictionary of atmospheric patterns using Latent Dirichlet Allocation

Lucas Fery, Berengere Dubrulle, Berengere Podvin, Flavio Pons, Davide Faranda

► To cite this version:

Lucas Fery, Berengere Dubrulle, Berengere Podvin, Flavio Pons, Davide Faranda. Learning a weather dictionary of atmospheric patterns using Latent Dirichlet Allocation. *Geophysical Research Letters*, 2022, 49, pp.e2021GL096184. <10.1029/2021GL096184>. <hal-03258523>

HAL Id: hal-03258523

<https://hal.science/hal-03258523v1>

Submitted on 11 Jun 2021

HAL is a multi-disciplinary open access archive for the deposit and dissemination of scientific research documents, whether they are published or not. The documents may come from teaching and research institutions in France or abroad, or from public or private research centers.

L'archive ouverte pluridisciplinaire **HAL**, est destinée au dépôt et à la diffusion de documents scientifiques de niveau recherche, publiés ou non, émanant des établissements d'enseignement et de recherche français ou étrangers, des laboratoires publics ou privés.



Distributed under a Creative Commons CC BY 4.0 - Attribution - International License

Learning a weather dictionary of atmospheric patterns using Latent Dirichlet Allocation

Lucas Fery^{1,2}, Berengere Dubrulle³, Berengere Podvin⁴, Flavio Pons¹, and Davide Faranda^{1,5,6,*}

¹Laboratoire des Sciences du Climat et de l'Environnement, CEA Saclay l'Orme des Merisiers, UMR 8212 CEA-CNRS-UVSQ, Université Paris-Saclay & IPSL, 91191, Gif-sur-Yvette, France

²Department of Physics, Ecole Normale Supérieure de Lyon, 69364, Lyon, France

³SPEC, CEA, CNRS, Université Paris-Saclay, F-91191 CEA Saclay, Gif-sur-Yvette, France

⁴LISN, CNRS, Université Paris-Saclay, 91405, Orsay, France

⁵London Mathematical Laboratory, 8 Margravine Gardens, London, W6 8RH, UK

⁶LMD/IPSL, Ecole Normale Supérieure, PSL research University, 75005, Paris, France

*daveide.faranda@lscce.ipsl.fr

ABSTRACT

Mid-latitude circulation dynamics is often described in terms of weather regimes, represented by atmospheric field configurations extracted using pattern recognition techniques. Each pattern is given by a given combination of distinct elements, corresponding to synoptic objects (cyclones and anticyclones). Such intrication makes it arduous to detect or quantify shifts in atmospheric circulation - possibly due to anthropogenic forcings - impacting recurrence and intensity of climate extremes. Here we apply Latent Dirichlet Allocation (LDA), typically used for topic modeling in linguistic studies, to build a weather dictionary: in analogy with linguistics, we define daily maps of a gridded target observable as documents, and the grid-points composing the map as words. LDA provides a representation of documents in terms of a combination of spatial patterns named *motifs*, which are latent patterns inferred from the set of snapshots. For atmospheric data, we find that *motifs* correspond to pure synoptic objects (cyclones and anticyclones), that can be seen as building blocks of weather regimes. We show that LDA weights provide a natural way to characterize the impact of climate change on the recurrence of regimes associated with extreme events.

Introduction

Describing mid-latitude atmospheric circulation is challenging because of the turbulent¹ and chaotic² nature of the underlying flow, driven by the jet stream³. The phase space of general turbulent geophysical flows is usually thought to be very large, with its dimension scaling as the Reynolds number⁴. However, previous work based on dimensionality reduction methods⁵ have shown that the mid-latitude dynamics can, in fact, be understood through a limited number of degrees of freedom, such as superpositions of cyclonic and anticyclonic structures in observable fields, like sea-level pressure or geopotential height⁶⁻⁸. Indeed, while cyclones and anticyclones normally progress West to East transported by the jet, they can sometimes organize in persistent or intense structures⁹. These structures yield to extreme events such as cold spells, heat waves or extratropical storms, whose frequency can be modified by anthropogenic forcing¹⁰. At first, the characterization of these patterns was based on atmospheric indices built upon physical arguments. For example, the North Atlantic Oscillation¹¹ or the Arctic Oscillation have been devised with the goal of separating blockings from the zonal flow. Later, unsupervised pattern recognition based on classification or dimensionality reduction methods, such as *k*-means¹², empirical orthogonal functions¹³ or proper orthogonal decomposition¹⁴, have allowed the detection of patterns (weather regimes¹⁵) in arbitrary situations. Such patterns can be used to separate modes of natural weather variability from extreme events and, sometimes with open debates, detect the effects of climate change^{16,17}. However, those methods provide a field description of patterns, made of a given combination of distinct elements, corresponding to synoptic objects (cyclones and anticyclones) : e.g. the NAO+ pattern includes both the Azores anticyclone and the Icelandic low pressure system. In a changing climate, shifts in these patterns are difficult to detect or analyse, as it is difficult to disentangle changes due to shifts in the synoptic objects properties, or shifts in their relative weights. Similarly, a description based on entire fields fails to identify the genesis and dynamical properties of extreme weather events, as the latter are often associated with specific cyclonic or anticyclonic structures. In addition, we point out that each field can only belong to a single cluster with the *k*-means method.

In this manuscript, we offer a change of perspective on atmospheric pattern recognition by adapting a machine learning technique used in linguistics to geophysical flows. Recently, several efforts have been made to apply machine learning to the

38 prediction of geophysical data¹⁸, to learn parameterizations of subgrid processes in climate models^{19–27}, to the forecasting^{28–31}
 39 and nowcasting (i.e. extremely short-term forecasting) of weather variables^{32–34}, and to quantify the uncertainty of deterministic
 40 weather prediction³⁵. We specifically use a soft clustering technique called Latent Dirichlet Allocation (LDA), a generative
 41 probabilistic model usually applied to collections of discrete data³⁶. In particular, LDA is widely used to describe *corpora* of
 42 text documents: each *document* is assumed to be a mixture of a small number of *topics* which are characterized by a distribution
 43 over *words* of a finite vocabulary. Here, we apply LDA to a set of daily sea-level pressure anomaly maps over North-Atlantic
 44 from 1948 to 2018, considering grid-points as the equivalent of words and looking for a classification of the pressure anomaly
 45 maps in terms of distinct patterns equivalent to the topics, as presented in Fig. 1. We show that LDA is capable to write
 46 any sea-level pressure map (*documents*) from the dataset (*corpus*) in terms of well-known cyclonic or anticyclonic structures
 47 (*motifs*, which are here the equivalent of *topics*). We choose here to think in terms of *motifs* instead of *topics* as these latent
 48 variables correspond to spatial patterns in our case. First, we show that building a weather dictionary requires a number of
 49 motifs compatible with the estimate of the number of active degrees of freedom of the gridded fields; this quantity should be
 50 ideally known prior to the application of LDA, and thus estimated with different techniques. Then, we show the usefulness of
 51 this mid-latitude weather dictionary to detect trends in occurrence of certain motifs caused by anthropogenic forcing and to find
 52 common precursors of different class of climate extremes, an important element to assess their predictability.

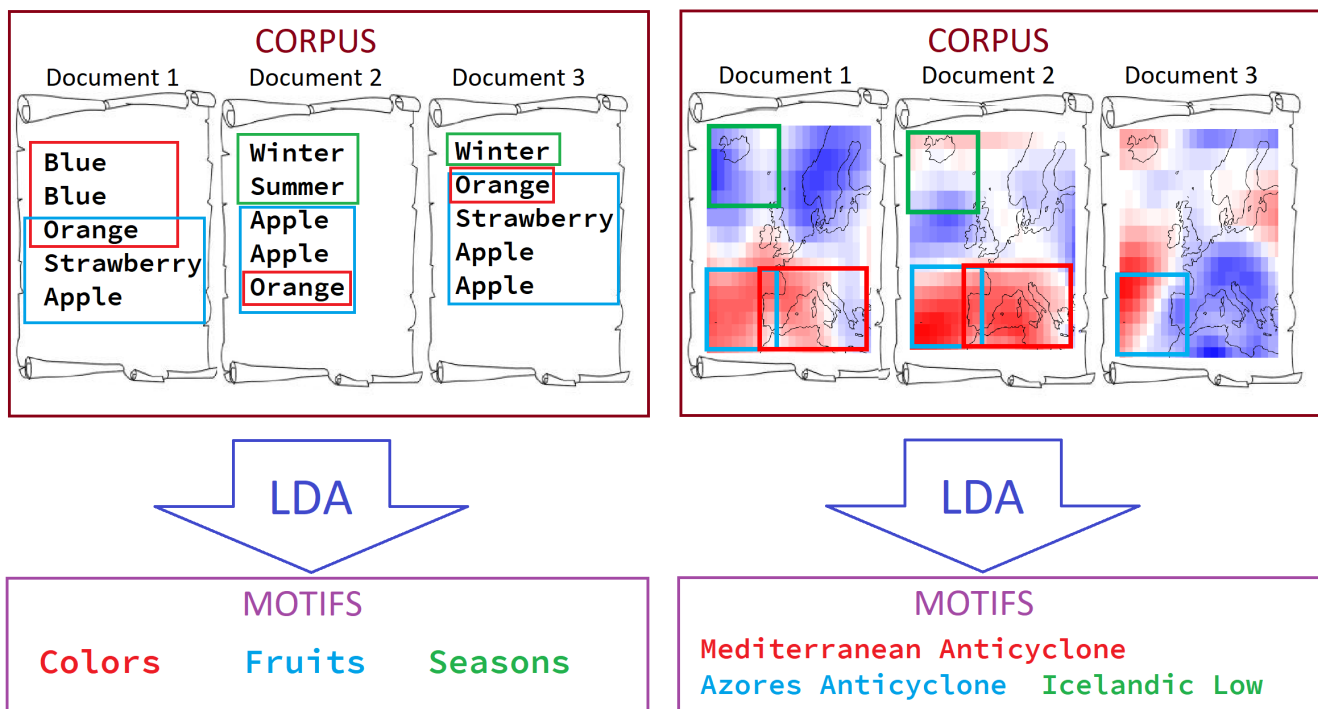


Figure 1. Diagram showing the analogy between the application of LDA to text documents and to a gridded observable map – here sea level pressure anomaly data. The equivalent of words in the latter case are the grid-points of the map and the value of the observable on the grid-points corresponds to the number of occurrences of the words. LDA identifies latent motifs – or topics in the case of text documents – in a corpus of documents that are defined by a distribution over the words of a finite vocabulary (see Methods for a detailed explanation), and then interpreted as meaningful patterns (e.g. “Colors”, “Fruits” and “Seasons” for the text documents or “Mediterranean Anticyclone”, “Azores Anticyclone” and “Icelandic low” for sea level pressure maps). Each word of the vocabulary, or equivalently each grid-point, can be associated with different motifs as represented by the word “orange” that can be seen as a fruit or a color.

53 Results

54 When applying LDA, one first needs to select the number of motifs that will be necessary to describe the whole dataset. Other
 55 pattern recognition methods allow to chose the optimal number of components, if this is not know a priori: for example, the
 56 scree plot defined by deviance within groups for k-means, or the proportion of explained variance for PCA. For LDA, we
 57 propose two measures : the relative area covered by the motifs and the motifs average area (see eqs. (6) and (7) in Methods).

58 We observe that these two metrics converge with an increasing number of motifs (see Fig.S1 and S2). Moreover, the length
 59 scale computed from the average area corresponds to the typical diameter of cyclones and anticyclones. This preliminary
 60 inspection suggests that taking 28 motifs is sufficient to get relevant patterns which are representative of the dynamics of
 61 mid-latitude circulation. This value is in very good agreement with the upper bound of the number of degrees of freedom
 62 obtained computing the local attractor dimensions for the same dataset³⁷. This suggests that each motif corresponds to an
 63 active degree of freedom in the maps, reinforcing the claim that cyclones and anticyclones are the building blocks of the
 64 dynamics of mid-latitude flows. This may also indicate that LDA could be a method more suitable than others to define the
 65 modes of variability associated with the number of active degrees of freedom estimated by the local dimension. The latter can
 66 indeed provide a suggestion for optimal dimensionality reduction, but does not provide a method to project the dataset on the
 67 reduced dimension. The 28 motifs obtained by training the LDA model on the daily sea-level pressure anomaly maps over
 68 North-Atlantic from 1948 to 2018 are presented in Fig.2 (see Methods for more details). First, we observe that they consist of
 69 localized anomaly patterns which are mostly exclusively positive or negative, with a radius between 1000 and 2000 km i.e. they
 70 truly correspond to cyclonic or anticyclonic anomalies. Furthermore, they reproduce the typical locations of pressure structures
 71 previously named by meteorologists studying North Atlantic circulation, e.g. the Genoa low (motif 8), the Icelandic low (motif
 72 18), the Siberian high (motif 3) or the Azores anticyclone (motif 7). This strengthens our confidence that the motifs are not only
 73 a practical way to represent a complex map, but also that they correspond to actual coherent sea level pressure patterns.

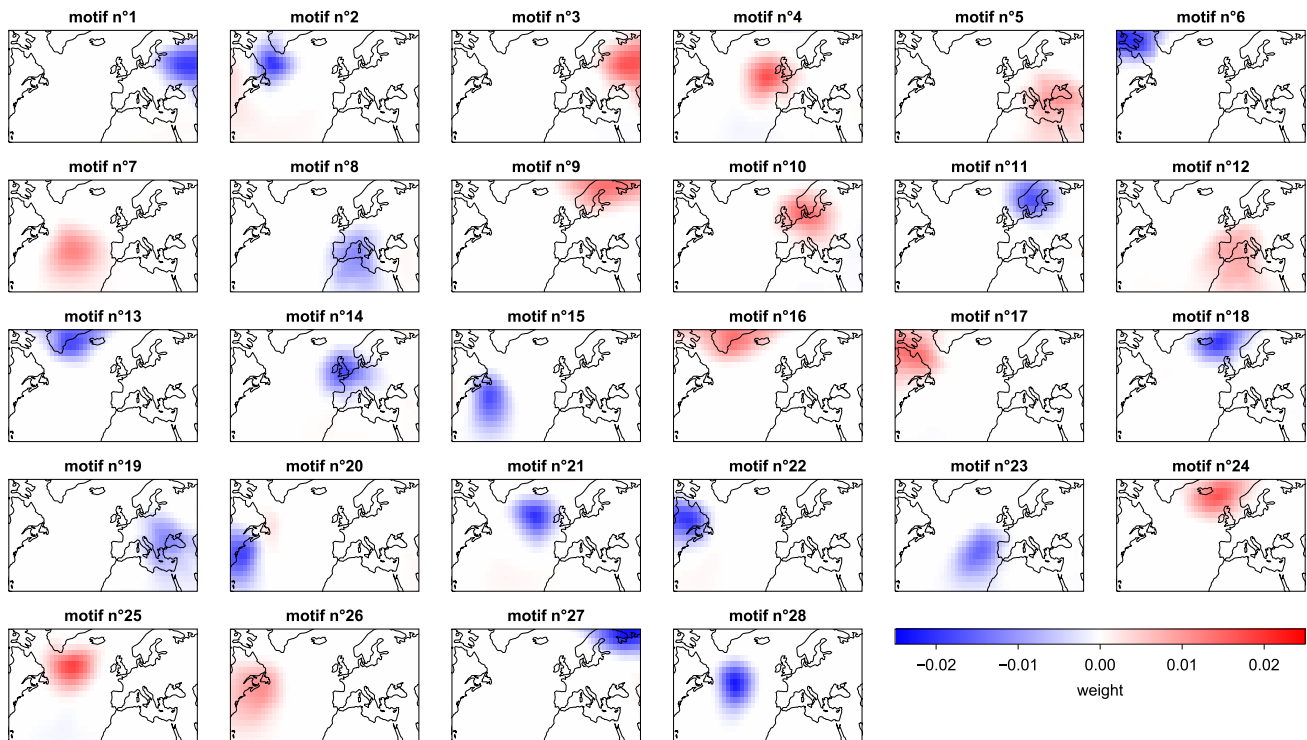


Figure 2. The 28 motifs identified by LDA by using as documents the daily sea-level pressure anomaly maps over North-Atlantic from 1948 to 2018. Positive anomalies and negative anomalies are respectively represented in red and blue. LDA outputs normalized topics, so the color intensity only represents a relative weight.

74 Internal variability and climate change

75 As each daily anomaly is represented by a mixture of motifs with given weights, we can study the evolution over years of
 76 the weight for each motif. The average values of the motifs weights for yearly intervals are presented in Fig.3. Most of the
 77 motifs show oscillations of weights of the order of few percents with signs alternating with interdecadal frequency, coherently
 78 with the claim that chaotic behaviour of mid-latitude circulation at climate scales dominate. On the contrary, motifs 5, 8, 12
 79 and 19 stand out with a visible coherent evolution over time. They correspond to pressure structures over Mediterranean sea.
 80 Anticyclonic anomalies associated with motifs 5 and 12 have been already linked to heatwaves on the Mediterranean basin^{38,39}.
 81 During the analysed period, there is an increase of high pressure patterns average weights and a corresponding decrease of low
 82 pressure ones. The augmented weight of motifs 5 and 10 could be explained via the strengthening of subtropical anticyclones

83 to higher latitudes and a corresponding weakening low pressure systems (motifs 8 and 19). This phenomenon, investigated in⁴⁰
 84 at the global scale, has received little attention for the Mediterranean basin, although few signals are coherent with our findings,
 85 namely the fact that this area will be warmer and dryer⁴¹, and that heatwaves are projected to increase^{42,43}.

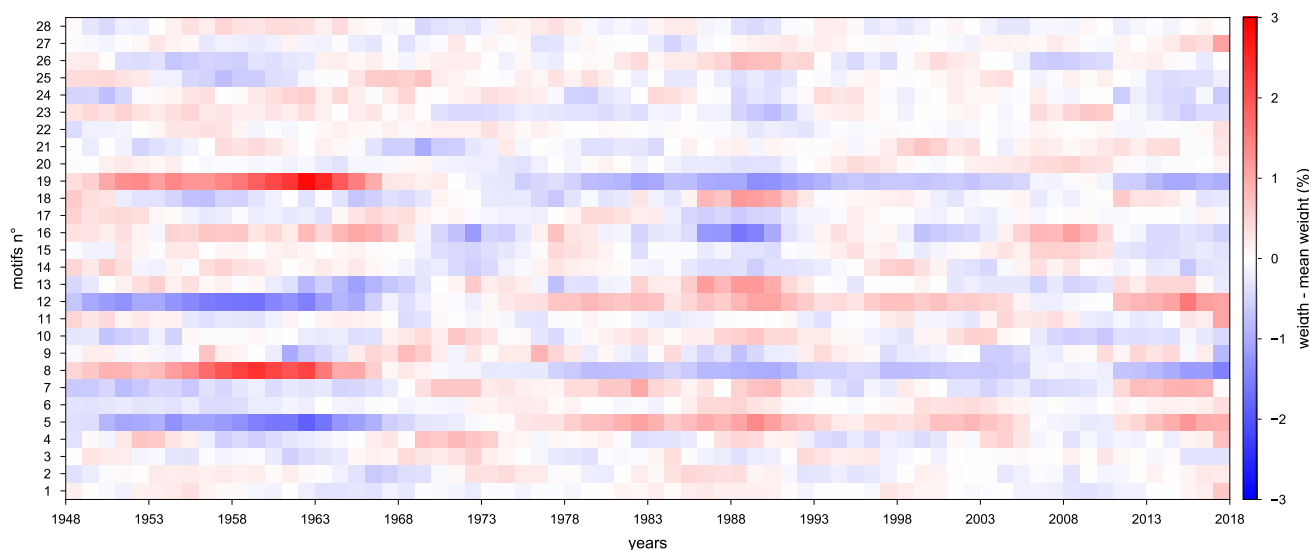


Figure 3. Evolution of mean motifs weights over the years. Each column corresponds to a time slot of one year from 1948 to 2018 and each row corresponds to a motif. The color represents the difference of the average weight of the time slot and the average weight over the whole interval. It is red if the weight is higher than the overall average and blue instead. We notice that at least four motifs differentiate themselves by a coherent evolution over time (motifs 5, 8, 12 and 19). They correspond to structures on Mediterranean sea, with an increase of high pressure patterns average weights and a decrease of low pressure ones.

86 Extreme events

87 We also investigate the distribution on motifs for particular events such as heat waves, cold waves and extra-tropical storms
 88 which are associated with large scale pressure anomaly patterns. We use the EM-DAT⁴⁴ database to identify these events and
 89 analyse their average properties in the motifs representation. This analysis has two main goals: first identify the relevant motifs
 90 for each class of extreme events and then verify whether some of the motifs are precursors of those extreme events. Note that
 91 the extreme events identified by EM-DAT are defined on the basis of their impacts and not by applying extreme value theory or
 92 statistical analysis of atmospheric variables. It is therefore interesting to see whether such extremes are associated to specific
 93 motifs⁴⁵. Fig.4, S12 and S13 each show the average anomaly map (e) and motifs weights (d) along with the corresponding
 94 three leading motifs (a,b,c) for 5 days before the beginning of the event (1), 3 days before (2), and on the first day of the event
 95 as reported in the EM-DAT databases (3) for the 3 types of events mentioned before. The distributions on the motifs for the first
 96 day (3) highlight the fact that we can identify dominant motifs that are consistent with each type of event. Indeed, we find
 97 positive anomalies i.e. high pressures for heat waves and cold waves, and negative anomalies i.e. low pressure for extra-tropical
 98 storms, as expected. What's more, this representation might shed light on teleconnections between different patterns^{46,47}. As
 99 an example Fig.S12 shows that heat waves on Europe tend to be associated with high pressure over Canada (motif 26). This
 100 teleconnection is a robust feature already identified with other techniques such as importance sampling⁴⁸. We also notice that
 101 LDA is capable of identifying motifs that act as precursors for these events. Let us analyse in details the case of cold-spells
 102 (Fig.4 and S10), for which motifs 9 and 24 are precursors several days in advance. These motifs show that cold spells over
 103 Europe are generally associated with anticyclonic blocking conditions located to the North of continental Europe, consistently
 104 with previous results⁴⁹. Looking at 5 days precursors of heat waves (Fig. S9 and S12), a cyclonic mid-Atlantic pattern appears.
 105 This is consistent with previous analysis⁵⁰ showing that a wavy pattern of wave number 7 with alternating cyclonic-anticyclonic
 106 structures favor heatwaves over Europe⁵¹.

107 Discussion

108 We have discussed the application of an unsupervised pattern recognition method based on Latent Dirichlet Allocation (LDA), a
 109 generative probabilistic model for collections of discrete data. The method has been applied to a set of snapshots featuring daily

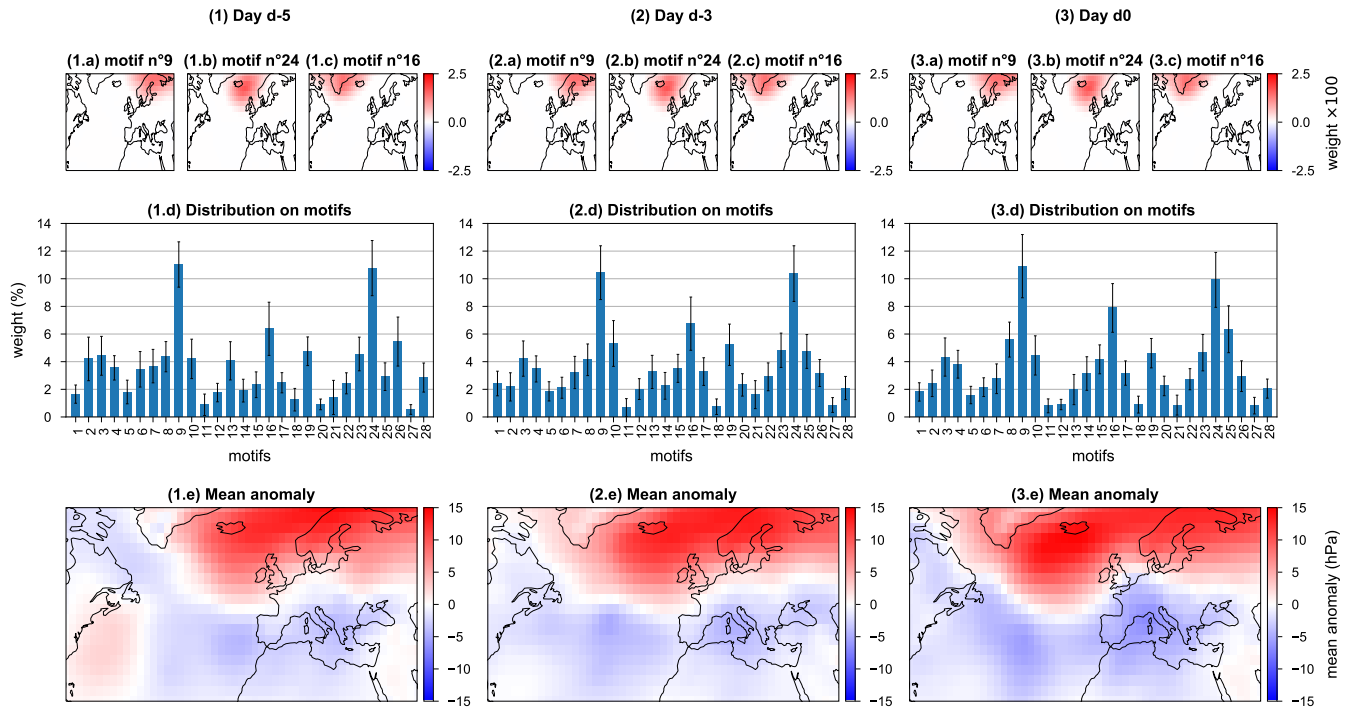


Figure 4. Mean anomaly for cold waves over Europe. The anomaly is presented for five days before the event (1), 3 days before (2) and on the first day of the event as identified in EM-DAT (3). (a-b-c) shows the three leading motifs in the LDA representation of the anomaly for the corresponding day. (d) shows the whole representation of the anomaly based on a weight assigned to each motif. (e) shows the mean anomaly map the corresponding events in the EM-DAT database. The error bars represent 2 times the standard error.

110 sea level pressure anomaly over North-Atlantic from 1948 to 2018. The main advantage of LDA is the representation of a map
 111 of a gridded observable in terms of a combination of motifs, which are latent spatial elements inferred from the set of snapshots.
 112 We have shown that the motifs correspond to intelligible localized patterns in contrast with other techniques¹²⁻¹⁴ like those
 113 leading to the definition of weather regimes¹⁵. Indeed motifs correspond to single cyclonic or anticyclonic patterns and are,
 114 therefore, of immediate interpretation for meteorologists and climatologists. Using motifs as a weather dictionary, we have
 115 been able to naturally address questions about climate change and precursors of weather extreme events which have required
 116 advanced analyses techniques in other studies^{8,9,39}. Our illustrative analysis of the capabilities of LDA for climate science has
 117 shown that subtle changes in the frequency or intensity of cyclonic structures over the Mediterranean can be distinguished from
 118 the general interdecadal variability of the chaotic atmospheric circulation. Furthermore, we have determined that only a few
 119 number of motifs are relevant to describe weather extreme events such as cold spells, heat waves or extratropical storms even if
 120 these have been defined only on the bases of their impacts in the EM-DAT database. This suggests a partially positive answer to
 121 the question raised by van der Wiel⁴⁵ on whether extreme events defined by their impacts can be connected to the underlying
 122 climate dynamics: the connection exists but with specific motifs rather than with maxima or minima of meteorological variables.
 123 We have also been able to identify precursors of these events through motifs and explain their origin, consistently with previous
 124 results⁴⁹⁻⁵¹.

125 Our study paves the way for several exciting applications of LDA in the context of present and future climates, namely i) a
 126 comprehensive study of precursors of extreme events, whose existence hints to a possibly unexploited predictive power of LDA
 127 ii) the intercomparison of climate models using as skill score their ability of representing specific motifs, e.g. those relevant for
 128 weather extreme events, iii) the analysis of the emergence or disappearance of motifs in different climates conditions.

129 Methods

130 We use daily sea level pressure data from NCEP/NCAR reanalysis⁵² over the period 01/01/1948 – 06/01/2018 ($S = 25,574$ days).
 131 The data is mapped on a ($m = 20, n = 53$) grid of resolution $2.5^\circ \times 2.5^\circ$ representing a region from 80W to 50E and 22.5N to

132 70N which corresponds to North Atlantic and Europe. We compute the daily seasonal standards of sea level pressure based on
 133 these data for every day of a year and then the daily anomaly by subtracting it to the original map. We then split each anomaly
 134 map into a positive anomaly map and a negative one. which is equivalent to doubling the size of the grid (or grid-points). The
 135 anomaly map constitute a pair of 2D arrays where each element of the (m,n) array (or grid-point) is characterized by a positive
 136 value. In the LDA framework, each grid-point is considered to be a word of a vocabulary. As already done by Frihat⁵³ for the
 137 identification of coherent structures in turbulent channel flow, the positive value of each element is assimilated as the number of
 138 occurrences of the word found in each document, i.e. the anomaly map, to within a potential rescaling factor and a digitization.
 139 Here we took a rescaling factor of 1 for the raw sea level pressure anomaly in Pa and we also put a threshold value of 100 Pa
 140 to consider only significant anomalies and to speed-up the training of the model by reducing the word count of documents.
 141 We train the LDA model with its implementation in the Gensim Python library⁵⁴. The LDA model takes several parameters
 142 as arguments, such as the number of *passes* and *iterations* (we refer to Gensim LDA documentation for a definition of these
 143 parameters). These have been chosen high enough so that the *perplexity*³⁶ – a quantity defined to evaluate the performance of
 144 the model – converges. Here we set the number of *iterations* as 2000, the number of *passes* as 20, the *chunksize* as 2048, *alpha*
 145 and *eta* as 'auto', *random state* as 100 to get reproducible results and other parameters to defaults values. The number of *topics*
 146 N is also a parameter which has to be set before training.

147 The program produces two arrays corresponding in the text mining applications to the *document-topic distributions* w (1)
 148 and the *topic-word distributions* t (2) which are normalized probability distributions. Thus, each document – here corresponding
 149 to a daily anomaly map $(a_{i,j}^s)_{i,j}$ with $s \in [1, S]$ denoting the snapshot in the dataset and $i \in [1, m]$ and $j \in [1, n]$ indicating the
 150 rows and columns of the map – is associated with a combination of *topics* with given weights w_l^s where $l \in [1, N]$ indicates the
 151 corresponding *topic*. Each *topic* t^l is defined the same way as a mixture of words of the vocabulary – i.e. grid-points of the
 152 positive and negative anomaly maps in our case – with given weights $t_{i,j,k}^l$ where $k \in \{+, -\}$ indicates the positive or negative
 153 map. We can thus think of topics as a normalized distribution on a set of two maps. We then combine the positive and negative
 154 maps of each *topic* to a single map which is interpreted as a spatial anomaly pattern that we call motif, which we represent
 155 by an array μ (3). From the *document-topic distribution* and the motifs, we can reconstruct the anomaly map to within a
 156 rescaling factor. To be able to compare the value of the reference anomaly a^s and the reconstructed one \hat{a}^s , we also multiply the
 157 combination of motifs by the sum of the reference absolute anomaly values on the whole map (4).

$$w = (w_l^s)_{l \in [1, N]}^{s \in [1, S]} \quad \text{with} \quad \forall (s, l), w_l^s \in [0, 1] \quad \text{and} \quad \forall s, \sum_l w_l^s = 1 \quad (1)$$

$$t = \left(t_{i,j,k}^l \right)_{i \in [1, m], j \in [1, n], k \in \{+, -\}}^{l \in [1, N]} \quad \text{with} \quad \forall (l, i, j, k), t_{i,j,k}^l \in [0, 1] \quad \text{and} \quad \forall l, \sum_{i,j,k} t_{i,j,k}^l = 1 \quad (2)$$

$$\mu = \left(\mu_{i,j}^l \right)_{i \in [1, m], j \in [1, n]}^{l \in [1, N]} \equiv \left(t_{i,j,+}^l - t_{i,j,-}^l \right)_{i \in [1, m], j \in [1, n]}^{l \in [1, N]} \quad (3)$$

$$\hat{a}^s \equiv \left(\sum_{i,j} |a_{i,j}^s| \right) \left(\sum_l w_l^s \mu^l \right) \quad (4)$$

158 As we want to find an optimal number of motifs, we consider the following indicators : the relative area covered by the
 159 motifs (7) and the motifs average area (6). To do so, we define the area A^l of a motif l by the number of elements of t^l (or
 160 grid-points of the pair of maps) whose values are above a threshold, parametrized by a coefficient $\alpha \in [0, 1]$ (5). Here we take
 161 $\alpha = 2/3$ to get values of area close to the value one would get by counting the colored pixels on the maps of motifs in Fig.
 162 2. On the one hand, Figure S1 shows that $r_c(\mu)$ increases and reaches about 99% at $N = 28$. Thus, we choose to consider
 163 $N = 28$ motifs for further analysis as taking more motifs would not improve significantly the coverage of the map by the motifs.
 164 Moreover, Figure S2 shows that $A(\mu)$ decreases and converges near 100 grid-points which corresponds to the typical diameter
 165 (2000-3000 km) of cyclones and anticyclones⁵⁵. This choice is further motivated by an independent analysis on the same
 166 dataset with a dynamical system angle³⁷. Indeed, this value of N is in very good agreement with the upper bound of the number
 167 of active degrees of freedom obtained computing the local attractor dimensions.

$$A^l = \text{card} \left\{ t_{i,j,k}^l \mid t_{i,j,k}^l > \max_{i,j,k} \{ t_{i,j,k}^l \} - \alpha \left(\max_{i,j,k} \{ t_{i,j,k}^l \} - \min_{i,j,k} \{ t_{i,j,k}^l \} \right) \right\} \quad \text{and} \quad \alpha \in [0, 1] \quad (5)$$

$$A(\mu) = \frac{1}{l} \sum_l A^l \quad (6)$$

$$r_c(\mu) = \frac{A_c(\mu)}{2mn} = \frac{1}{2mn} \text{card} \left\{ (i, j, k) \mid \exists l \in [1, N], t_{i,j,k}^l > \max_{i,j,k} \{t_{i,j,k}^l\} - \alpha \left(\max_{i,j,k} \{t_{i,j,k}^l\} - \min_{i,j,k} \{t_{i,j,k}^l\} \right) \right\} \quad (7)$$

References

- 168
- 169 **1.** Marino, R., Pouquet, A. & Rosenberg, D. Resolving the paradox of oceanic large-scale balance and small-scale mixing. *Phys. review letters* **114**, 114504 (2015).
- 170
- 171 **2.** Lorenz, E. N. Deterministic nonperiodic flow. *J. atmospheric sciences* **20**, 130–141 (1963).
- 172 **3.** Hilborn, R. C. Sea gulls, butterflies, and grasshoppers: A brief history of the butterfly effect in nonlinear dynamics. *Am. J. Phys.* **72**, 425–427 (2004).
- 173
- 174 **4.** Dubrulle, B., Daviaud, F., Faranda, D., Marié, L. & Saint-Michel, B. Lewis fry richardson medal lecture – how many modes are needed to predict climate bifurcations ? : Lessons from an experiment. *Nonlin. Process. Geophys. Discuss.* (2021). Preprint at <https://doi.org/10.5194/npg-2021-19>.
- 175
- 176
- 177 **5.** Gámez, A. J., Zhou, C., Timmermann, A. & Kurths, J. Nonlinear dimensionality reduction in climate data. *Nonlinear Process. Geophys.* **11**, 393–398 (2004).
- 178
- 179 **6.** Rivière, G., Arbogast, P., Lapeyre, G. & Maynard, K. A potential vorticity perspective on the motion of a mid-latitude winter storm. *Geophys. Res. Lett.* **39** (2012).
- 180
- 181 **7.** Shepherd, T. G. Atmospheric circulation as a source of uncertainty in climate change projections. *Nat. Geosci.* **7**, 703 (2014).
- 182
- 183 **8.** Cassou, C. & Cattiaux, J. Disruption of the european climate seasonal clock in a warming world. *Nat. Clim. Chang.* **6**, 589 (2016).
- 184
- 185 **9.** Ferranti, L., Corti, S. & Janousek, M. Flow-dependent verification of the ecmwf ensemble over the euro-atlantic sector. *Q. J. Royal Meteorol. Soc.* **141**, 916–924 (2015).
- 186
- 187 **10.** Rummukainen, M. Changes in climate and weather extremes in the 21st century. *Wiley Interdiscip. Rev. Clim. Chang.* **3**, 115–129 (2012).
- 188
- 189 **11.** Folland, C. K. *et al.* The summer north atlantic oscillation: past, present, and future. *J. Clim.* **22**, 1082–1103 (2009).
- 190 **12.** Vrac, M. & Yiou, P. Weather regimes designed for local precipitation modeling: Application to the mediterranean basin. *J. Geophys. Res. Atmospheres* **115** (2010).
- 191
- 192 **13.** Zampieri, M., Toreti, A., Schindler, A., Scoccimarro, E. & Gualdi, S. Atlantic multi-decadal oscillation influence on weather regimes over europe and the mediterranean in spring and summer. *Glob. Planet. Chang.* **151**, 92–100 (2017).
- 193
- 194 **14.** Wang, Z., Akhtar, I., Borggaard, J. & Iliescu, T. Proper orthogonal decomposition closure models for turbulent flows: a numerical comparison. *Comput. Methods Appl. Mech. Eng.* **237**, 10–26 (2012).
- 195
- 196 **15.** Vautard, R. Multiple weather regimes over the north atlantic: Analysis of precursors and successors. *Mon. weather review* **118**, 2056–2081 (1990).
- 197
- 198 **16.** Cohen, J. *et al.* Recent arctic amplification and extreme mid-latitude weather. *Nat. geoscience* **7**, 627 (2014).
- 199 **17.** Screen, J. A. The missing northern european winter cooling response to arctic sea ice loss. *Nat. communications* **8**, 14603 (2017).
- 200
- 201 **18.** Wu, J.-L., Xiao, H. & Paterson, E. Physics-informed machine learning approach for augmenting turbulence models: A comprehensive framework. *Phys. Rev. Fluids* **3**, 074602 (2018).
- 202
- 203 **19.** Krasnopolsky, V. M., Fox-Rabinovitz, M. S. & Chalikov, D. V. New approach to calculation of atmospheric model physics: Accurate and fast neural network emulation of longwave radiation in a climate model. *Mon. Weather. Rev.* **133**, 1370–1383 (2005).
- 204
- 205
- 206 **20.** Krasnopolsky, V. M. & Fox-Rabinovitz, M. S. Complex hybrid models combining deterministic and machine learning components for numerical climate modeling and weather prediction. *Neural Networks* **19**, 122–134 (2006).
- 207

- 208 **21.** Rasp, S., Pritchard, M. S. & Gentine, P. Deep learning to represent subgrid processes in climate models. *Proc. Natl. Acad. Sci.* **115**, 9684–9689 (2018).
- 209
- 210 **22.** Gentine, P., Pritchard, M., Rasp, S., Reinaudi, G. & Yacalis, G. Could machine learning break the convection parameterization deadlock? *Geophys. Res. Lett.* **45**, 5742–5751 (2018).
- 211
- 212 **23.** Brenowitz, N. D. & Bretherton, C. S. Prognostic validation of a neural network unified physics parameterization. *Geophys. Res. Lett.* **45**, 6289–6298 (2018).
- 213
- 214 **24.** Brenowitz, N. D. & Bretherton, C. S. Spatially extended tests of a neural network parametrization trained by coarse-graining. *J. Adv. Model. Earth Syst.* **11**, 2728–2744 (2019).
- 215
- 216 **25.** Yuval, J. & O’Gorman, P. A. Stable machine-learning parameterization of subgrid processes for climate modeling at a range of resolutions. *Nat. communications* **11**, 1–10 (2020).
- 217
- 218 **26.** Gettelman, A. *et al.* Machine learning the warm rain process. *J. Adv. Model. Earth Syst.* **13**, e2020MS002268 (2021).
- 219 **27.** Krasnopolsky, V. M., Fox-Rabinovitz, M. S. & Belochitski, A. A. Using ensemble of neural networks to learn stochastic convection parameterizations for climate and numerical weather prediction models from data simulated by a cloud resolving model. *Adv. Artif. Neural Syst.* **2013** (2013).
- 220
- 221
- 222 **28.** Liu, J. N., Hu, Y., He, Y., Chan, P. W. & Lai, L. Deep neural network modeling for big data weather forecasting. In *Information Granularity, Big Data, and Computational Intelligence*, 389–408 (Springer, 2015).
- 223
- 224 **29.** Grover, A., Kapoor, A. & Horvitz, E. A deep hybrid model for weather forecasting. In *Proceedings of the 21th ACM SIGKDD International Conference on Knowledge Discovery and Data Mining*, 379–386 (ACM, 2015).
- 225
- 226 **30.** Haupt, S. E. *et al.* Machine learning for applied weather prediction. In *2018 IEEE 14th International Conference on e-Science (e-Science)*, 276–277 (IEEE, 2018).
- 227
- 228 **31.** Weyn, J. A., Durran, D. R. & Caruana, R. Can machines learn to predict weather? using deep learning to predict gridded 500-hpa geopotential height from historical weather data. *J. Adv. Model. Earth Syst.* **11**, 2680–2693 (2019).
- 229
- 230 **32.** Xingjian, S. *et al.* Convolutional lstm network: A machine learning approach for precipitation nowcasting. In *Advances in neural information processing systems*, 802–810 (2015).
- 231
- 232 **33.** Shi, X. *et al.* Deep learning for precipitation nowcasting: A benchmark and a new model. In *Advances in neural information processing systems*, 5617–5627 (2017).
- 233
- 234 **34.** Sprenger, M., Schemm, S., Oechslin, R. & Jenkner, J. Nowcasting foehn wind events using the adaboost machine learning algorithm. *Weather. Forecast.* **32**, 1079–1099 (2017).
- 235
- 236 **35.** Scher, S. & Messori, G. Predicting weather forecast uncertainty with machine learning. *Q. J. Royal Meteorol. Soc.* (2018).
- 237 **36.** Blei, D. M., Ng, A. Y. & Jordan, M. I. Latent dirichlet allocation. *J. machine Learn. research* **3**, 993–1022 (2003).
- 238 **37.** Faranda, D., Messori, G. & Yiou, P. Dynamical proxies of north atlantic predictability and extremes. *Sci. reports* **7**, 1–10 (2017).
- 239
- 240 **38.** Stefanon, M., D’Andrea, F. & Drobinski, P. Heatwave classification over europe and the mediterranean region. *Environ. Res. Lett.* **7**, 014023 (2012).
- 241
- 242 **39.** Alvarez-Castro, M. C., Faranda, D. & Yiou, P. Atmospheric dynamics leading to west european summer hot temperatures since 1851. *Complexity* **2018** (2018).
- 243
- 244 **40.** Li, W., Li, L., Ting, M. & Liu, Y. Intensification of northern hemisphere subtropical highs in a warming climate. *Nat. Geosci.* **5**, 830–834 (2012).
- 245
- 246 **41.** Drobinski, P. *et al.* How warmer and drier will the mediterranean region be at the end of the twenty-first century? *Reg. Environ. Chang.* **20**, 1–12 (2020).
- 247
- 248 **42.** Bador, M. *et al.* Future summer mega-heatwave and record-breaking temperatures in a warmer france climate. *Environ. Res. Lett.* **12**, 074025 (2017).
- 249
- 250 **43.** Perkins-Kirkpatrick, S. & Gibson, P. Changes in regional heatwave characteristics as a function of increasing global temperature. *Sci. Reports* **7**, 1–12 (2017).
- 251
- 252 **44.** CRED, D. G.-S. Em-dat: The emergency events database. www.emdat.be. Université catholique de Louvain (UCL), Brussels, Belgium.
- 253
- 254 **45.** van der Wiel, K., Selten, F. M., Bintanja, R., Blackport, R. & Screen, J. A. Ensemble climate-impact modelling: extreme impacts from moderate meteorological conditions. *Environ. Res. Lett.* **15**, 034050 (2020).
- 255

- 256 **46.** Agarwal, A. *et al.* Network-based identification and characterization of teleconnections on different scales. *Sci. reports* **9**,
257 1–12 (2019).
- 258 **47.** Wazneh, H., Gachon, P., Laprise, R., de Vernal, A. & Tremblay, B. Atmospheric blocking events in the north atlantic:
259 trends and links to climate anomalies and teleconnections. *Clim. Dyn.* 1–23 (2021).
- 260 **48.** Ragone, F., Wouters, J. & Bouchet, F. Computation of extreme heat waves in climate models using a large deviation
261 algorithm. *Proc. Natl. Acad. Sci.* **115**, 24–29 (2018).
- 262 **49.** Raymond, F., Ullmann, A., Camberlin, P., Oueslati, B. & Drobinski, P. Atmospheric conditions and weather regimes
263 associated with extreme winter dry spells over the mediterranean basin. *Clim. Dyn.* **50**, 4437–4453 (2018).
- 264 **50.** Kornhuber, K. *et al.* Extreme weather events in early summer 2018 connected by a recurrent hemispheric wave-7 pattern.
265 *Environ. Res. Lett.* **14**, 054002 (2019).
- 266 **51.** Petoukhov, V., Rahmstorf, S., Petri, S. & Schellnhuber, H. J. Quasiresonant amplification of planetary waves and recent
267 northern hemisphere weather extremes. *Proc. Natl. Acad. Sci.* **110**, 5336–5341 (2013).
- 268 **52.** Kalnay, E. *et al.* The ncep/ncar 40-year reanalysis project. *Bull. Am. meteorological Soc.* **77**, 437–472 (1996).
- 269 **53.** Frihat, M., Podvin, B., Mathelin, L., Fraigneau, Y. & Yvon, F. Coherent structure identification in turbulent channel flow
270 using latent dirichlet allocation. *arXiv preprint arXiv:2005.10010*, accepted by *J. Fluid Mech.* (2021).
- 271 **54.** Řehůřek, R. & Sojka, P. Software Framework for Topic Modelling with Large Corpora. In *Proceedings of the LREC 2010*
272 *Workshop on New Challenges for NLP Frameworks*, 45–50 (ELRA, Valletta, Malta, 2010). [http://is.muni.cz/publication/](http://is.muni.cz/publication/884893/en)
273 [884893/en](http://is.muni.cz/publication/884893/en).
- 274 **55.** Ulbrich, U., Leckebusch, G. & Pinto, J. G. Extra-tropical cyclones in the present and future climate: a review. *Theor. Appl.*
275 *Climatol.* **96**, 117–131 (2009).

276 **Acknowledgements**

277 This work is supported by the CNRS INSU-LEFE-MANU grant "DINCLIC" and by the French ANR-T-ERC grant "BOREAS".
278 We thank Aglaé Jézéquel, Théo Mandonnet and the ESTIMR team for useful discussions.

279 **Author contributions**

280 D.F and B.D. conceived the study; L.F. performed all dynamical and statistical analyses by adapting the numerical code written
281 by B.P.; F.P. suggested statistical tests to check the robustness of the findings. All authors participated in writing and reviewing
282 the manuscript.

283 **Competing Interests**

284 The authors report no conflict of interest.

285 **Supplementary Information**

286 See detached document